541 (1966).
[2]R. H. Iyer and J. W. Cobble, Phys. Rev. 172, 1186 (1968).
[3]K. W. MacMurdo and J. W. Cobble, Phys. Rev. 182, 1303, (1969).
[4]R. Gunnink and J. W. Cobble, Phys. Rev. 115, 1247 (1959); R. Gunnink, Ph.D. thesis, Purdue University, June 1959 (unpublished).
[5]Silver of 99.999% purity and aluminum of 99.99% purity were obtained from United Mineral and Chemical Company, New York, New York.
[6]Analysis carried out by National Spectrographic Laboratories, Inc., Cleveland, Ohio.
[7]Analyses carried out by Battelle Memorial Institute, Columbus, Ohio.
[8]T. C. Roginski, Ph.D. thesis, Purdue University, June 1970 (unpublished).
[9]L. J. Colby, Jr., and J. W. Cobble, Anal. Chem. 31, 798, (1959).
[10]L. J. Colby, Jr., and J. W. Cobble, Phys. Rev. 121, 1410, (1961).
[11]J. A. Powers, N. A. Wogman, and J. W. Cobble, Phys. Rev. 152, 1088 (1966).
[12]E. K. Hyde, *The Nuclear Properties of the Heavy Elements* (Prentice-Hall, Inc., Englewood Cliffs, New Jersey, 1964), Vol. III, pp. 153–155.
[13]N. Sugarman, H. Muzel, J. A. Panontin, K. Wielgoz, M. V. Raminiah, G. Lange, and E. Lopez-Menchero, Phys. Rev. 143, 952 (1966).
[14]S. Muskergee and L. Yaffe, Can. J. Chem. 43, 232 (1965).
[15]L. C. Northcliffe, Phys. Rev. 120, 1744 (1960).
[16]R. H. Iyer, C. K. Matthews, N. Ravindran, K. Rengan, D. V. Singh, M. V. Raminiah, and H. D. Sharma, J. Inorg. Nucl. Chem. 25, 465 (1963).
[17]L. J. Colby, Jr., M. L. Shoaf, and J. W. Cobble, Phys. Rev. 121, 1415 (1961).
[18]G. Friedlander, J. Kennedy, and J. Miller, *Nuclear and Radiochemistry* (John Wiley & Sons, Inc., New York, 1964), 2nd ed., pp. 44, 313–315.
[19]D. L. Uhl, Ph.D. thesis, Purdue University, January 1970 (unpublished).
[20]D. L. Uhl, T. L. McDaniel, and J. W. Cobble, preceding paper, Phys. Rev. C 4, 1357 (1971).

PHYSICAL REVIEW C VOLUME 4, NUMBER 4 OCTOBER 1971

# Study of Charge-Exchange Coupling in Proton-Induced Reactions on $^{95,98,100}$Mo and $^{92,94}$Zr†

R. A. Hinrichs,* G. W. Phillips,‡ J. G. Cramer, and H. Wieman
*Nuclear Physics Laboratory, University of Washington, Seattle, Washington 98105*

(Received 2 June 1971)

The presence of isospin coupling in the incident channel has been studied via proton-induced reactions on $^{95,98,100}$Mo and $^{92,94}$Zr. Anomalous behavior in the excitation functions at backward angles was observed in deuteron and proton outgoing channels. In the deuteron channels these anomalies, located near the $(p,n)$ threshold to the ground-state analog, were, for almost all cases, similarly characterized by a double-dipped shape. Their strength is generally much weaker than the single minima observed in $(d,p)$ reactions near mass 90 and can be categorized by the proton decay energy from the analog state formed in the charge-exchange process. The proton elastic excitation functions showed no structure near the $(p,n)$ thresholds although the $(p,p')$ curves did exhibit fluctuations.

## I. INTRODUCTION

The observation of charge-exchange effects in single-nucleon-transfer reactions has been the subject of considerable study in recent years. Such effects were initially observed by Moore *et al.*[1] as an anomaly (dip or cusp) in the backward-angle $^{90}$Zr$(d,p)^{91}$Zr(g.s.) excitation function, centered about the threshold energy of the $(d,n)$ channel to the isobaric analog state (IAS) in $^{91}$Nb. Similar isospin coupling effects have been observed in many other nuclei, especially around $A \approx 90$. The absence of such phenomena in other mass regions, or in transitions to particular states in the mass-90 region, has led to an understanding of the conditions necessary for the observation of such anomolies[2] and the explanation of the effect as due to coupling of the exit channel to the charge-exchange channel.

While the majority of such observations has been restricted to $(d,p)$ reactions, charge-exchange effects have also been observed[3,4] in the inverse $(p,d)$ reaction. In this case, under the assumption of a charge-exchange process, there is coupling between the proton-plus-target channel and the virtual, neutron-plus-target analog channel. As illustrated in Fig. 1, the neutron in this latter channel can pick up a proton from the IAS and form a deuteron, leaving the residual nucleus in its ground state or in an excited state. The energy at which

the charge-exchange channel opens is the $(p,n)$ threshold to the IAS of the target nucleus. Since the coupling is in the entrance channel, anomalous behavior would be expected in all outgoing channels. This paper describes a study of isospin coupling in proton-induced reactions on several nuclei, for which evidence is presented for the observation of anomalies in several outgoing channels in the vicinity of the $(p,n)$ threshold to the IAS. The origins of and trends in such behavior are discussed.

## II. THEORETICAL BACKGROUND

With the inclusion of a charge-dependent term $\vec{t}\cdot\vec{\tau}$ in the Schrödinger equation, the matrix element for the $(d,p)$ reaction can be written[5] (in the zero-range approximation) as

$$T_{(d,p)} = \langle X_p^{(-)}\phi_n | V_{np} | X_d^{(+)}\rangle - \frac{1}{(2T+1)^{1/2}}\langle X_n^{(-)}\phi_p | V_{np} | X_d^{(+)}\rangle . \quad (1)$$

Here the $X^{(-)}$ are solutions of the Lane equations, $X_d^{(+)}$ is the normal deuteron distorted wave, $\phi_n$ is the usual bound-state wave function, and $\phi_p$ is the (propagating) wave function of a proton in the IAS. A coupled-channel analysis with this reformulated matrix element has been carried out by Coker and Tamura[2] and Tamura and Watson[6] on some of the Zr and Mo isotopes and has successfully fit the general shape of the observed anomalies. The partial-wave scattering matrix elements obtained in these coupled-channel calculations show a strong energy dependence in the neutron $p$ wave near the threshold. The responsibility of this feature for the anomaly appears understandable as $A \approx 90$ is in the region of the neutron $p$-wave strength function. To observe isospin coupling in this region, the deuteron energy should be near the Coulomb barrier, as contributions from higher partial waves would wash out the effect of the $p$-wave resonances; this results in the condition[2] that $Q(d,p) \gtrsim \frac{1}{4}\Delta_C$, $\Delta_C$ being the Coulomb-energy difference.

Tables I and II list most of the $(d,p)$ and $(p,d)$ reactions studied to date, with information as to the qualitative "strength" of the anomaly observed, the $Q$ value of the reaction, and the energy available for proton decay from the IAS formed in the $(d,n)$ or $(p,n)$ reaction ($E_{\bar{p}}$). Trends are observable in this data, as will be discussed further in Secs. IV and V.

## III. EXPERIMENTAL PROCEDURE AND RESULTS

These experiments were performed with a proton beam from the University of Washington FN tandem Van de Graaff. The energy-analyzed beam was focused into a 60-in. (diameter) scattering chamber in which the target and detectors were positioned. The beam entered the chamber through a $\frac{3}{16}$-in. collimator and $\frac{1}{4}$-in. clean-up aperture. A smaller aperture ($\frac{3}{32}$ in.), that could be remotely inserted into the beam, allowed for easy focusing of the beam on target at each energy of an excitation function. The reaction products produced in the $(p,d)$, $(p,t)$, and $(p,p')$ reactions were detected by a thermoelectrically cooled $\Delta E$-$E$ detector-telescope system. The energy signals were amplified, fed to an ORTEC 423 particle-identifier unit, and then into an XDS 930 on-line computer system. A two-parameter particle-identification program was used to sort the pulses into energy spectra of 1024 channels, corresponding to windows set with a light pen for the different particle peaks in the identifier spectrum. The targets used were all self-supporting metal foils,[7] of about 1 mg/cm$^2$.

TABLE I. Charge-exchange investigations for the $(d,p)$ reaction.

| Tgt. | To state | $E_d^{(c.m.)}$ | $Q(d,p)$ | $\frac{1}{4}\Delta_C$ | $E_{\bar{p}}$ | Strength of anomaly | References |
|---|---|---|---|---|---|---|---|
| $^{90}$Zr | $d_{5/2}$ | 6.89 | 4.98 | 2.98 | 4.70 | Strong | 1 |
| $^{91}$Zr | $0^+$ | 5.42 | 6.42 | 2.96 | 3.20 | Very weak | 14, 15 |
| $^{91}$Zr | $2^+$ (0.934) | 6.35 | 5.49 | 2.96 | 4.13 | Weak | 14, 15 |
| $^{91}$Zr | $4^+$ (1.49) | 6.91 | 4.93 | 2.96 | 4.69 | Strong | 14, 15 |
| $^{92}$Zr | $d_{5/2}$ | 7.31 | 4.50 | 2.95 | 5.09 | Strong | 13 |
| $^{94}$Zr | $d_{5/2}$ | 7.43 | 4.24 | 2.92 | 5.20 | Strong | 13 |
| $^{92}$Mo | $d_{5/2}$ | 6.61 | 5.83 | 3.11 | 4.30 | Weak | 13 |
| $^{94}$Mo | $d_{5/2}$ | 7.14 | 5.15 | 3.07 | 4.83 | Strong | 13 |
| $^{89}$Y | $2^-$ | 6.88 | 4.67 | 2.89 | 4.65 | Weak | 17 |
| $^{52}$Cr | $p_{3/2}$ | 2.68 | 5.72 | 2.10 | 0.46 | Weak | 18 |
| $^{80}$Se | $p_{1/2}$ | 5.72 | 4.59 | 2.58 | 3.60 | Very weak | 19 |
| $^{88}$Sr | $d_{5/2}$ | 6.74 | 4.55 | 2.82 | 4.90 | Strong | 20 |
| $^{40}$Ar | $f_{7/2}$ | 2.71 | 3.88 | 1.65 | 0.49 | Weak | 21 |

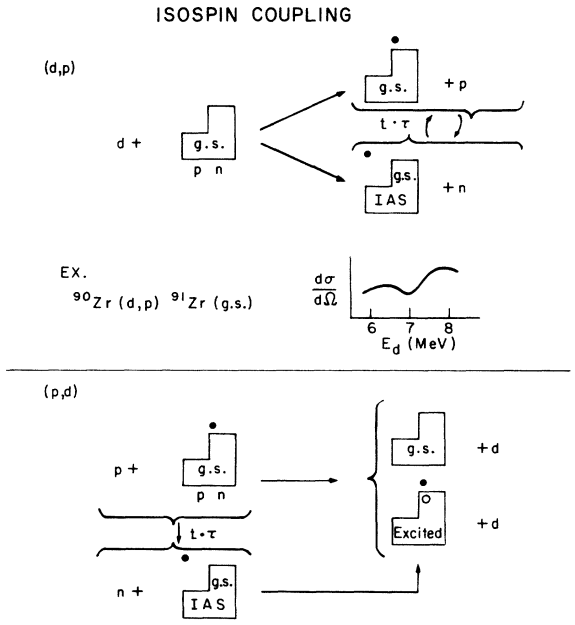


FIG. 1. Pictorial diagram illustrating the effect of isospin coupling in $(d,p)$ and $(p,d)$ reactions.

### A. $^{98}$Mo + $p$

Excitation functions for the reactions $(p,d)$, $(p,t)$, and $(p,p')$ were taken on $^{95,98,100}$Mo and $^{92,94}$Zr at an angle of 160 or 165°. The reaction $^{98}$Mo + $p$ was the first example studied and has been reported in part previously.[3] The $^{98}$Mo target was chosen because kinematics allowed observation of outgoing deuterons to many excited states in $^{97}$Mo, and also $A = 98$ lies in the region of the peak of the $p$-wave neutron strength function, as is the case of the Zr isotopes used in $(d,p)$ studies.

The $^{98}$Mo + $p$ excitation functions were taken at 165° with proton bombarding energies between 11.0 and 14.2 MeV. Figure 2 shows the cross sections for the $(p,d)$ reaction to the first three strongly excited states in $^{97}$Mo: the $d_{5/2}$ ground state $(d_0)$, the $g_{7/2}$ 0.667-MeV state $(d_1)$ – actually a triplet of states, and the $d_{3/2}$ 1.27-MeV state $(d_2)$. The $(p,n)$ threshold is at the lab energy of 12.21 MeV (first arrow in figure). In the $^{98}$Mo$(p,d_0)$ reaction, definite structure is observed in the excitation function at this threshold, with no other fluctuations of comparable size observed over the 3-MeV interval. There is also some subthreshold structure which can be characterized as a rise in the curve some 200 keV below threshold, with a flattening out or dip at the threshold.

The $(p,d_1)$ and $(p,d_2)$ excitation functions also show weak anomalous interference-like behavior near the $(p,n)$ threshold, appearing to be due to charge-exchange effects in the entrance channel. Although wiggles are seen in both of these channels at energies not connected with an apparent threshold, the dips in the $d_0$ and $d_1$ channels at 12.2 MeV have quite similar shapes with all three curves displaying the common feature of a dip about 200 keV below threshold. (The letters in the figure label the anomalies as they will be compared later.)

Charge-exchange effects of a somewhat more complicated type can also be present at the $(p,n)$ threshold leading to the IAS of the $2^+$ first excited state of $^{98}$Mo, located at 12.99 MeV (arrow). (This corresponds to the threshold for quasi-inelastic excitation of the vibrational $2^+$ state.) In this region of the excitation functions, no cross-section variations are apparent in the $d_0$ channel, but there is evidence of cross-section fluctuations in the $d_1$ and $d_2$ channels with double-dip shapes similar to those observed at the quasielastic threshold. This characteristic shape and the 200-keV width of the structure, in contrast to narrower wiggles present elsewhere in the excitation function, strongly suggest the presence of charge-exchange effects at this energy. The data for these excitation functions were reproduced in two different runs. The energy resolution was about 15 keV and the width $\Gamma$ of the nuclear states in this region and at this energy in the compound nucleus (20–23 MeV) has been measured to be less than 1 keV.[8]

This more complicated behavior is particularly interesting in that it would occur through isospin

TABLE II. Charge-exchange investigations for the $(p,d)$ reaction.

| Tgt. | To state | $E_p^{(c.m.)}$ | $Q(p,d)$ | $\frac{1}{4}\Delta_C$ | $E_{\bar{p}}$ | $E_d$ | References |
|---|---|---|---|---|---|---|---|
| $^{96}$Zr | $d_{5/2}$ | 11.61 | −5.61 | 2.90 | 3.80 | 6.03 | 4 |
| $^{94}$Zr | $d_{5/2}$ | 11.69 | −6.00 | 2.91 | 3.46 | 5.75 | Present |
| $^{92}$Zr | $d_{5/2}$ | 11.78 | −6.42 | 2.95 | 3.14 | 5.36 | Present |
| $^{91}$Zr | $0^+$ | 11.89 | −4.98 | 2.98 | 4.70 | 6.91 | 22 |
| $^{98}$Mo | $d_{5/2}$ | 12.14 | −6.42 | 3.04 | 3.53 | 5.72 | 3 |
| $^{98}$Mo | $g_{7/2}$ (0.67) | 12.14 | −7.09 | 3.04 | 3.53 | 5.05 | 3 |
| $^{98}$Mo | $d_{3/2}$ (1.27) | 12.14 | −7.69 | 3.04 | 3.53 | 4.45 | 3 |
| $^{95}$Mo | $0^+$ | 12.29 | −5.15 | 3.07 | 4.83 | 7.14 | Present |
| $^{100}$Mo | $s_{1/2}$ | 12.06 | −6.08 | 3.02 | 3.76 | 5.98 | Present |

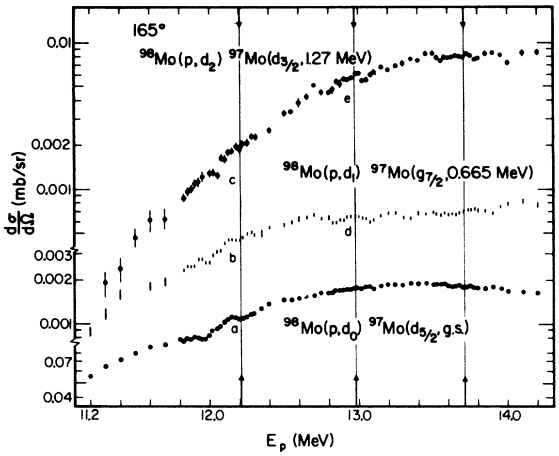


FIG. 2. $^{98}$Mo$(p,d)$ excitation functions at 165° to first three strongly excited states in $^{97}$Mo. The arrows correspond to $(p,n)$ thresholds to the isobaric analogs of the ground, $2^+$ (0.78-MeV) and $2^+$, $4^+$ (1.49-MeV) states of $^{98}$Mo.

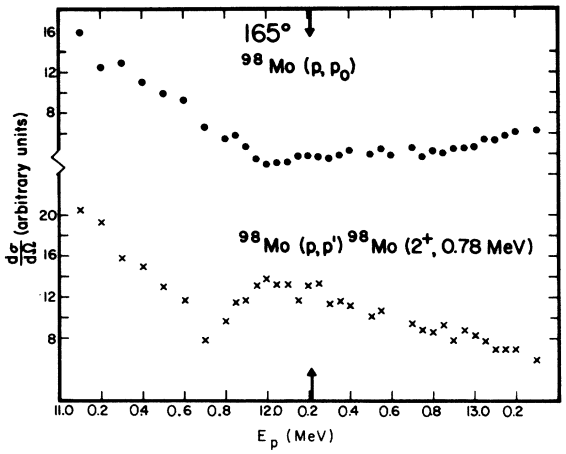


FIG. 4. Excitation functions at 165° for elastic scattering and inelastic scattering from the first excited $2^+$ state in $^{98}$Mo. The arrows correspond to the $(p,n)$ thresholds as explained in Fig. 2.

coupling to a channel which is what we might call "nonanalogous" to the incident channel, as for example, the virtual, neutron-plus-$^{98}$Tc$^A(2^+)$ channel. (The superscript $A$ is used to denote the isobaric analog of the target state in parenthesis, usually the ground state.) From a spectroscopic viewpoint this is the equivalent of protons bombarding an excited target and would allow the study of states in the residual nucleus which have the configuration of a hole coupled to an excited state of the target core. Such coupling to nonanalogous channels can be explained by using a deformed isospin potential with terms $Y_l^m$ of order at least $l=2$. Such an effect is most likely to be observable when the excited state of the target has a large probability of collective excitation. At the threshold (13.70 MeV) for quasi-inelastic scattering to the IAS of the $2^+$, $4^+$ doublet in $^{98}$Mo, there is no clear evidence of charge-exchange effects.

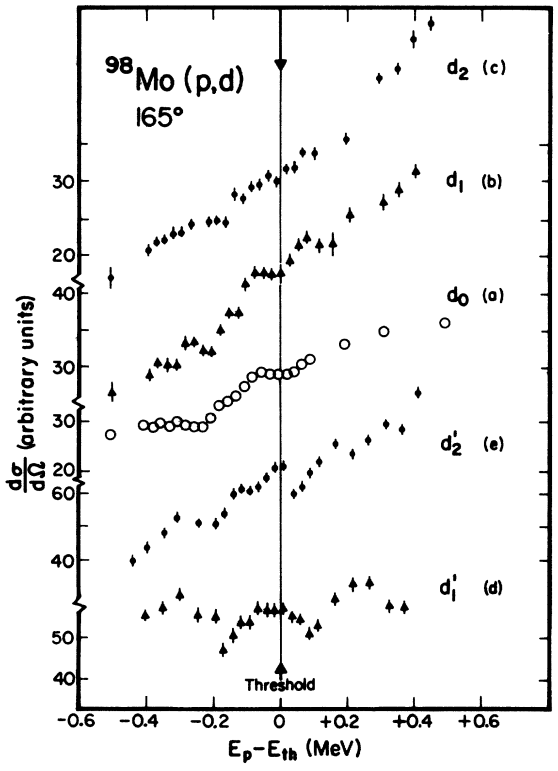


FIG. 3. Portions of the $^{98}$Mo$(p,d)$ excitation curves with $(p,n)$ thresholds for the ground- and first-excited-state analogs aligned. The letters (a)–(e) refer to the particular portions of the excitation curves as labeled in Fig. 2.

Figure 3 shows portions of the $(p,d)$ excitation curves with the $(p,n)$ thresholds for the ground and first excited states aligned. The curves are plotted as a function of energy from threshold in order to illustrate some of the aforementioned similarities in the different channels. These shapes, as characterized by a double dip in the cross section, differ markedly from the single-minimum shapes observed previously in $(d,p)$ reactions and calculated by Tamura and Watson.[6]

Figure 4 shows the proton elastic and inelastic excitation functions on $^{98}$Mo. The elastic curve is quite smooth, except for a small dip at 12.0 MeV. In the excitation function for the $(p,p')$ reaction to the $2^+$ state at 0.78 MeV in $^{98}$Mo there is some structure in the vicinity of the $(p,n)$ threshold. The cross section increases by some 50% about 400 keV below the threshold, decreasing smoothly above. This structure does not appear to be at the exact energies of the dips in the $(p,d)$ curves but, as we shall see later, similar behavior is evident in the inelastic scattering for the other isotopes

studied. In previous searches for the effect of the $(p,n)$ threshold upon proton elastic scattering, experiments on $^{91}$Zr and $^{40}$Ca[9] and on $^{56}$Fe, $^{55}$Mn, and $^{63,65}$Cu[10] have yielded negative results. This is in agreement with Tamura and Watson[6] who showed that the anomaly in the $(d,p)$ cases arises from large effects in the neutron wave function, in this case for the $l=1$ partial wave. The proton wave function is only slightly affected by the coupling. As elastic proton scattering may be dominated by Coulomb effects which include a large number of partial waves and are not directly sensitive to the coupling between the analog channels, inelastic scattering may be a more sensitive test. One might expect to see coupling effects in $(p,p')$ both at the $(p,n)$ threshold to the ground state, corresponding to charge exchange in the incident channel, and possibly also at the $(p,n)$ threshold to the excited-state analog, corresponding to an exit-channel effect. There appears to be evidence of the former case here.

Another possible interpretation of the observed structure in the outgoing channels is that they are due to the formation of compound-nuclear states through the incident channel. A correlation of fluctuations in several outgoing channels would indicate they were compound nuclear in origin. One such case is the formation of IAS resonances in the entrance channel.[11] In this case such structure would result from the excitation of an analog state in $^{99}$Tc. As the energy of a proton necessary to reach an analog state is given by $E_p = \Delta_C - B_n$, where $B_n$ is the binding energy of the neutron state in $^{99}$Mo, this is the analog of a state in $^{99}$Mo with $B_n \approx 0$. Such fluctuations have been observed in other nuclei (for example in $^{96}$Zr[4]) although the widths are typically much smaller than the 100–200 keV observed in these experiments. However, as pointed out in the preceding paragraph, no resonance structure in the proton channel is apparent here at the appropriate energies, thus reducing the possibility of IAS resonances being responsible for the structure observed in the $^{98}$Mo$(p,d)$ curves.

Excitation functions for $p+^{98}$Mo were also taken at 125°. These are shown in Fig. 5. The $(p,d_0)$ curve, over this limited energy range, is smooth except for a slight inflection near the threshold, similar to that for 165°. It was observed[12] in the $(d,p)$ excitation functions that the shape of the anomaly remained the same but its strength became much weaker at more-forward angles. This appears to be the situation here. Figure 12, which is displayed later, shows the curves of $^{98}$Mo$(p,d_0)$ at 165 and 125° together. One does not expect the shape of IAS resonance effects to remain the same with angle. The proton elastic and inelastic excitation functions at 125° showed no structure in this energy range.

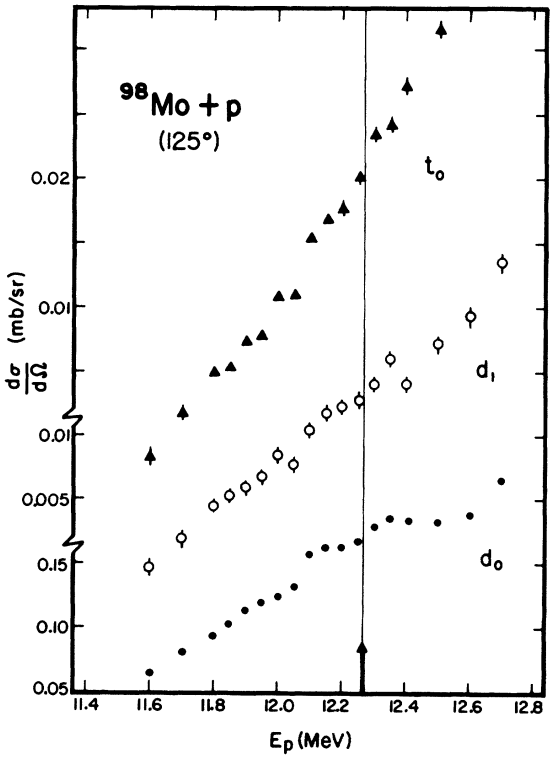


FIG. 5. Excitation functions at 125° for $^{98}$Mo$(p,d)$ to the ground and first excited states in $^{97}$Mo and for $^{98}$Mo$(p,t_0)$ to the ground state in $^{96}$Mo. The arrow denotes the $(p,n)$ threshold to the isobaric analog of the ground state.

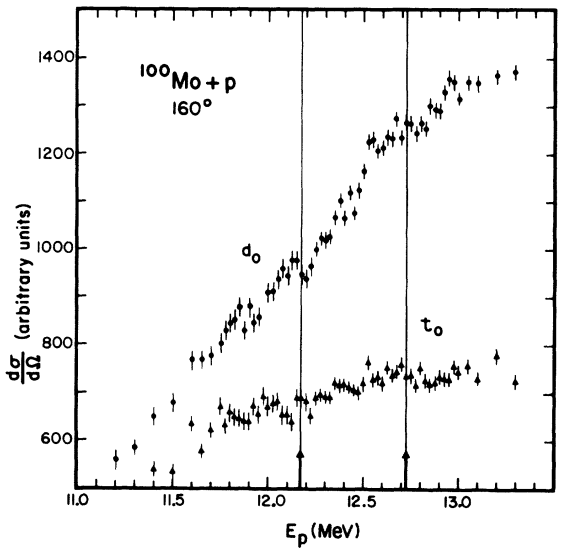


FIG. 6. $^{100}$Mo$(p,d_0)$ and $(p,t_0)$ excitation functions at 160° to the ground states in $^{99}$Mo and $^{98}$Mo. The arrows correspond to the $(p,n)$ thresholds to the isobaric analogs of the ground and $2^+$ (0.54 MeV) states of $^{100}$Mo.

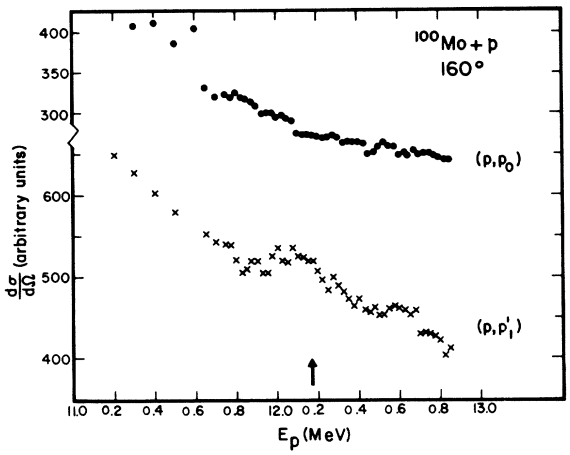


FIG. 7. Excitation functions at 160° for elastic scattering and inelastic scattering to the $2^+$ first excited state (0.54 MeV) in $^{100}$Mo. The arrow denotes the $(p,n)$ threshold to the isobaric analog of the ground state.

### B. $^{100}$Mo + $p$

Figure 6 shows $(p, d_0)$ and $(p, t_0)$ excitation functions at 160° for $^{100}$Mo between 11.2 and 13.3 MeV. The $(p, n)$ threshold is at $E_p^{lab} = 12.17$ MeV. Although statistical fluctuations are present, the $(p, d_0)$ curve shows dips at the $(p, n)$ threshold and 200 keV below, quite similar to the double-dip phenomena in $^{98}$Mo$(p, d)$. The inelastic scattering curve (Fig. 7) shows structure below the $(p, n)$ threshold, although weaker than that for $^{98}$Mo. The elastic curve is quite smooth.

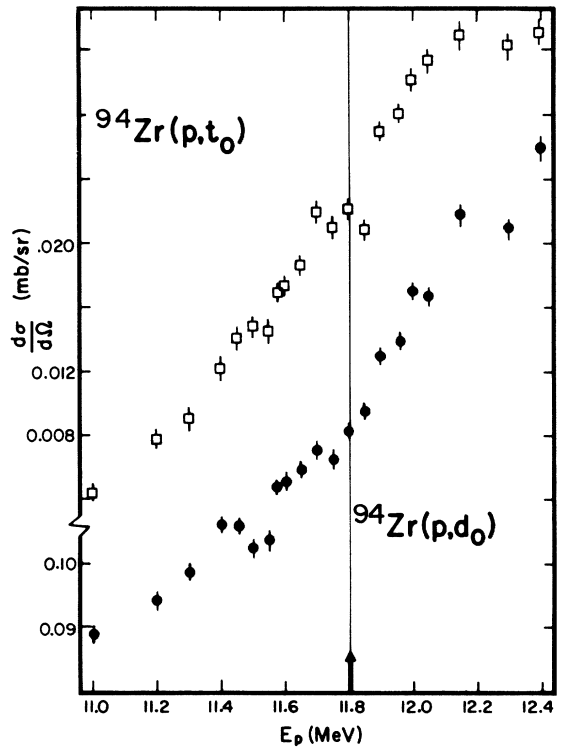


FIG. 8. $^{94}$Zr$(p,d_0)$ and $^{94}$Zr$(p,t_0)$ excitation functions at 165° to the ground states in $^{93}$Zr and $^{92}$Zr. The arrow denotes the $(p,n)$ threshold to the ground IAS.

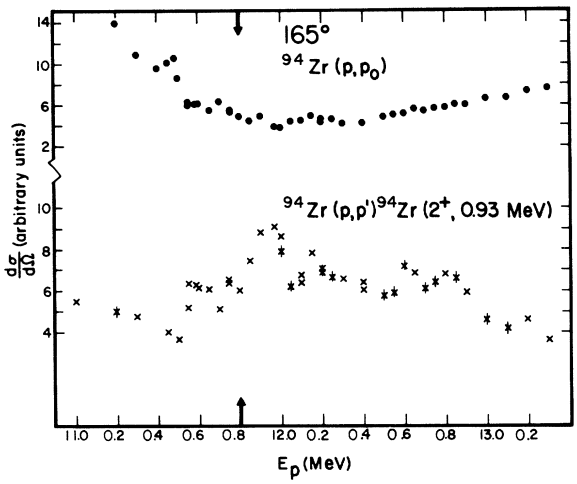


FIG. 9. Excitation functions at 165° for proton elastic scattering and inelastic scattering to the $2^+$ first excited state in $^{94}$Zr. The arrow denotes the $(p,n)$ threshold to the ground IAS.

### C. $^{94}$Zr + $p$

The excitation function for this reaction was taken at 165° over the energy range 11.0 to 13.3 MeV. Only deuterons and tritons to the ground states of $^{93}$Zr and $^{92}$Zr were strongly observed. Figure 8 shows the results up to 12.4 MeV. The $(p, n)$ threshold to the $^{94}$Nb$^A$(g.s.) is at $E_p^{lab} = 11.78$ MeV. There is little pronounced structure in both the $(p, d_0)$ and $(p, t_0)$ curves, although there is a dip in the $(p, d_0)$ curve several hundred keV below threshold as in $^{98}$Mo. In the $(p, d_0)$ curve at the 12.7-MeV quasi-inelastic threshold to the $2^+$ state (0.93 MeV), there were no signs of possible nonanalogous channel coupling, as there appeared to be for $^{98}$Mo. The proton elastic scattering in this energy region is quite smooth, although the $(p, p')$ cross section to the $2^+$ state does change rapidly below threshold as seen in Fig. 9.

### D. Other Nuclei

It was of interest to study incident-channel charge-exchange effects on odd-$A$ targets, with the $(p, d)$ reaction going to collective states. $^{95}$Mo was selected, with the $(p, d)$ threshold to the IAS at a lab energy of 12.39 MeV. Figure 10 shows the excitation functions for the $(p, d)$ reaction to the $^{94}$Mo ground state $(d_0)$, the $2^+$ first excited state at 0.87 MeV $(d_1)$, and the $2^+$, $4^+$ doublet at 1.57 MeV $(d_2)$. The $(p, d_0)$ excitation function ex-

hibits a substantially broad unsymmetric minimum centered at the $(p,n)$ threshold. The result is the same as that observed by Heffner *et al.*[13] for $^{94}$Mo$(d,p)^{95}$Mo(g.s.), as would be expected from time-reversal invariance. The data for $^{94}$Mo$(d,p)$ are shown on this figure as a dashed line normalized to the $(p,d_0)$ data. The ratio of the two cross sections is equal to that expected from detailed balance. The $(p,d_1)$ and $(p,d_2)$ curves show no apparent anomalies at this energy. The proton elastic scattering excitation function is smooth over this energy region; the inelastic scattering excitation function (to the first excited state) does show small fluctuations near threshold as seen in $^{94}$Zr and $^{98}$Mo.

The $(p,d_0)$ reaction on $^{92}$Zr was also studied with results similar to those already reported[14,15] for the $^{91}$Zr$(d,p)$ reaction. Weak fluctuations exhibiting the shape of a double dip are observed (Fig. 11). In work on nuclei in the region of the $s$-wave neutron strength function, the $^{140}$Ce$(p,d)$ reaction yielded no positive results. This was also true for the $(d,p)$ reaction on $^{140}$Ce,[13] where $Q=3.21$ MeV and $\frac{1}{4}\Delta_C=4.78$ MeV.

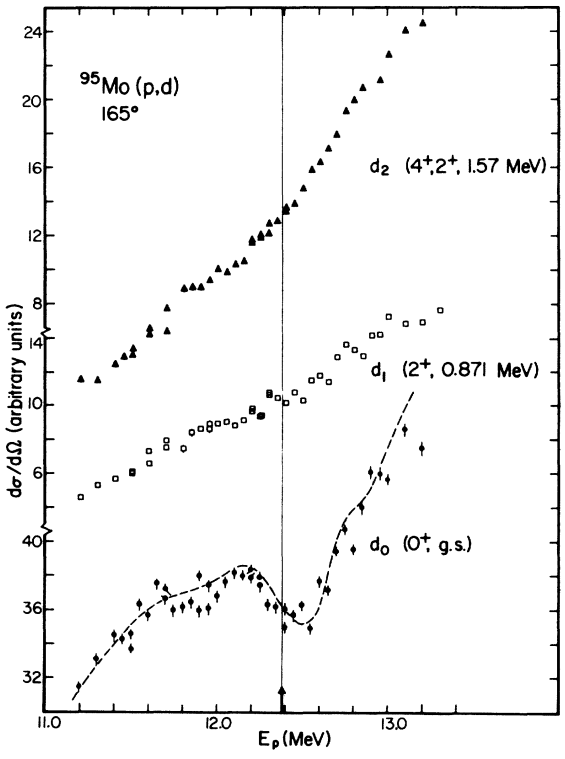


FIG. 10. $^{95}$Mo$(p,d)$ excitation curves at 165° to ground and first two excited states in $^{94}$Mo. The arrow corresponds to the $(p,n)$ threshold to the ground IAS of $^{95}$Mo. The dashed line in the $(p,d_0)$ curve represents the data for $^{94}$Mo$(d,p)$ of Ref. 13.

## IV. DISCUSSION

### A. Comparison of Present Results

The similarity of shapes observed in the $(p,d_0)$ excitation functions in the vicinity of the $(p,n)$ threshold is shown in Fig. 12, where the data for $^{98}$Mo (165 and 125°), $^{100}$Mo, and $^{94}$Zr are displayed with their $(p,n)$ thresholds aligned. Structure is evident in all these curves before and on the threshold, although the shape is not identical in every case. (It should be stated that evidence for the fluctuations, or anomalies, being nonstatistical in origin, is tentative in some cases studied and depends strongly on the feature of their similarities in shapes.)

The occurrence of these anomalous effects is attributed to isospin coupling in the incident channel because of the similarity of their shapes at different angles (and for different targets) and for the presence of fluctuations at excited IAS thresholds (or nonanalogous anomalies) for $^{98}$Mo, also with a shape similar to that of the ground-state anomaly. The proton elastic scattering excitation functions for $^{98,100}$Mo and $^{94}$Zr are smooth in the vicinity of the $(p,n)$ threshold, while the inelastic scattering curves do show broad fluctuations around this energy region, although not directly correlated with those dips observed in the $(p,d)$ curves. In the case of $^{96}$Zr$+p$, narrow fluctuations in both the proton elastic and inelastic scattering excitation functions led Michelman, Bonner, and Kulleck[4] to conclude that IAS resonance behavior in the proton channel was responsible for the

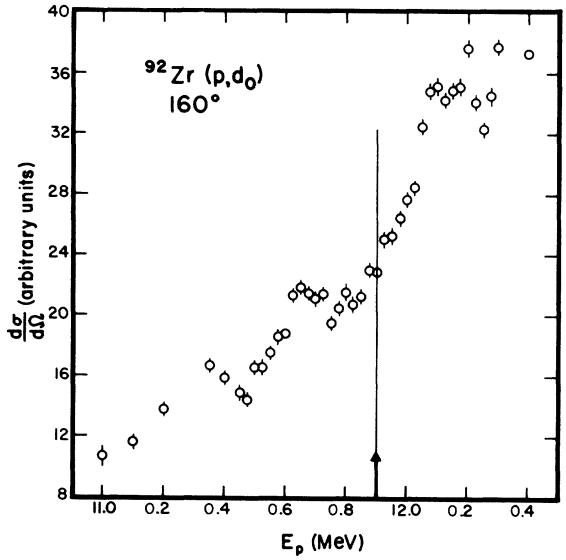


FIG. 11. $^{92}$Zr$(p,d)$ excitation function at 160° to the ground state of $^{91}$Zr. The arrow denotes the $(p,n)$ threshold to the ground IAS.

double dip observed in the $(p, d_0)$ curve. The above results do not support this conclusion in the present experiments.

### B. Comparison of $(p, d)$ and $(d, p)$ Anomalies

The anomalies observed in the $(d, p)$ and $(p, d)$ excitation functions appear to follow a $|Q| \geq \frac{1}{4}\Delta_C$ trend. One might also classify the anomalies through the energy of the unbound proton in the IAS. Equation (1) shows that the size of the exchange term is proportional to the overlap of the distorted neutron wave $X_n^{(-)}$ and that of the unbound proton in the IAS, $\phi_p$. For an energy higher in the potential well for the proton, $\phi_p$ will have a larger tail outside the nuclear radius past the Coulomb barrier, and therefore will increase the exchange term. Table I shows values for $E_{\bar{p}}$, the proton decay energy from the IAS. This energy is given (for $^{91}$Nb$^A$) by

$$E_{\bar{p}} = \Delta_C(^{91}\mathrm{Zr}) - B_n(^{91}\mathrm{Zr}). \quad (2)$$

It appears that $E_{\bar{p}}$ is an important quantity to know in understanding the trends of the anomalies. For the work on $^{91}$Zr$(d, p)$,[14] it was observed that the anomaly was strongest for stripping to the second excited $4^+$ state at 1.49 MeV and much weaker to the ground and first excited state. This anomaly occurred at a deuteron energy of about 7 MeV and its shape was almost identical to that seen in $^{90}$Zr$(d, p)^{91}$Zr$(d_{5/2})$. Moore concluded that the characteristics of the anomaly appear to be independent of the structure of the final state. This is consistent with the distorted-wave Born approximation where the structure of the final state enters only through the spectroscopic factor. An important point here is that $E_{\bar{p}}(^{91}\mathrm{Nb}^A(d_{5/2})) = 4.70$ and $E_{\bar{p}}(^{92}\mathrm{Nb}^A(4^+)) = 4.69$ MeV. For the lower excited states in $^{92}$Zr, this energy is less (see Table I). The origin of differences between the single dips observed in the $(d, p)$ excitation functions near the $(d, n)$ threshold and the structure of the $(p, d)$ excitation functions near the $(p, n)$ threshold seems to be found in the values of $E_{\bar{p}}$ (see Table II). For $^{94}$Mo$(d, p)$, $E_{\bar{p}} = 4.83$ MeV while for $^{98}$Mo$(p, d)$, $E_{\bar{p}} = 3.53$ MeV. Consequently, for the $(p, d)$ reactions considered, one would expect to find only small effects in the excitation function because of isospin coupling. The strength of any charge-exchange anomaly is proportional to the interference term found in the square of the matrix element of Eq. (1). In both the $(d, p)$ and $(p, d)$ cases only a few partial waves enter in the deuteron channel as the energies are near the Coulomb barrier. The effect of the resonant $l = 1$ neutron wave is thus enhanced in these situations. Comparing the $(p, d)$ results, one finds trends with the value of $E_{\bar{p}}$ for the different isotopes. For $^{98}$Mo, $E_{\bar{p}} = 3.53$ MeV, while for $^{92}$Zr, $E_{\bar{p}} = 3.14$ MeV (the very tenuous case). For $^{95}$Mo, $E_{\bar{p}} = 4.83$ MeV, considerably larger than for the even isotopes.

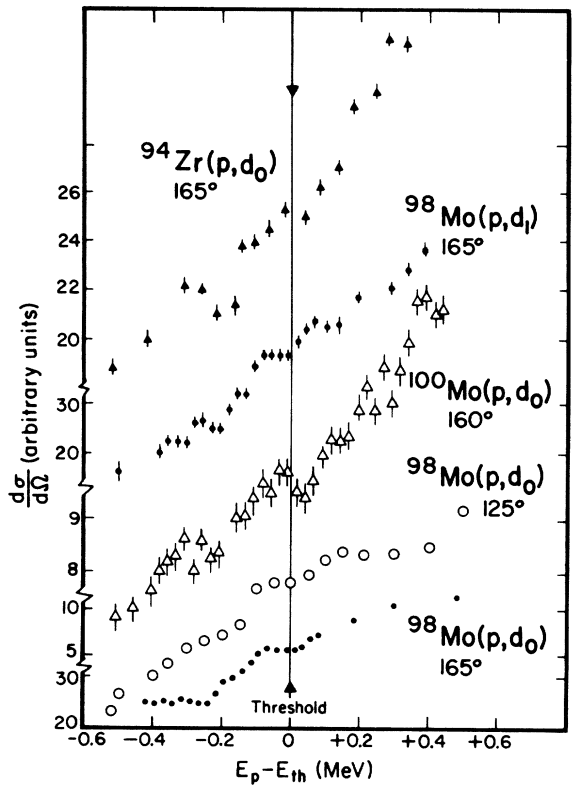


FIG. 12. Comparison of portions of $(p, d_0)$ excitation functions on $^{98,100}$Mo and $^{94}$Zr with their $(p, n)$ thresholds aligned.

### C. Recent Calculations

Lane has recently undertaken a study of the charge-exchange anomalies,[16] using elementary physical arguments. The assumption that the anomalies result from the occurrence of a single-particle $p$-wave state at zero energy and the interplay of this with the threshold leads to an expression for the $S$ matrix which involves a background term that includes all proton partial waves other than $l = 1$, and two resonance terms arising from the $p$-wave neutron state, split into its two spin-orbit components for $j = \frac{3}{2}$ and $\frac{1}{2}$. The features of the anomalies are reproduced quite well for the single-minimum $(d, p)$ dips; the double-dip shape of $^{98}$Mo$(p, d_0)$ is reproduced by allowing a variation in the strength and separation of the two spin-orbit amplitudes.

Lane also shows that the size and shape of the anomalies can be classified accurately by the $Q$ value. This is closely related to our $E_{\bar{p}}$ in the mass-90 region. Generalizing Eq. (2), for $(p, n)$

charge exchange on a mass-$A$ charge-$Z$ target followed by $\bar{p}$ decay of the IAS, we have

$$E_{\bar{p}} = \Delta_C(A,Z) - B_n(A,Z). \quad (3)$$

The $Q$ value for $(p,d)$ on the same target is

$$Q(p,d) = B_n(D) - B_n(A,Z),$$
$$= B_n(D) - \Delta_C(A,Z) + E_{\bar{p}}, \quad (4)$$

where the deuteron binding energy $B_n(D)$ is a constant and $\Delta_C$, which is proportional to $Z/A^{1/3}$, is nearly constant over the region of interest.

## V. CONCLUSION

Differential cross sections were measured at backward angles for proton-induced reactions on $^{95,98,100}$Mo and $^{92,94}$Zr at energies in the vicinity of the $(p,n)$ threshold to the IAS. The effects of charge exchange in the incident channel were observed, at least weakly, in all cases, the evidence being in the anomalous behavior of the $(p,d)$ excitation functions near this threshold. The shapes of the anomalies were similar in most all cases. For $^{98}$Mo$(p,d)$, anomalous behavior in the excitation functions for several outgoing deuteron channels was observed at the $(p,n)$ threshold to the IAS, and evidence for the same behavior was also found at the quasi-inelastic threshold to collective states. Structure was also observed at the $(p,n)$ threshold for $(p,p')$ scattering to the first excited state, although not in the proton elastic scattering. These effects are attributed to isospin coupling in the entrance channel, being observed as anomalies in the excitation functions in this mass region due to the resonating $l=1$ neutron partial wave. Such effects have previously been described, at least qualitatively for the cases studied, by either including a resonance term in the $S$ matrix that involves two terms arising from the $p$-wave neutron state or by using a coupled-channel calculation with a reformulated matrix element that arises from the inclusion of the charge-exchange term $\vec{t}\cdot\vec{\tau}$.

---

†Work supported in part by the U. S. Atomic Energy Commission.

*Present address: Cyclotron Laboratory, Michigan State University, East Lansing, Michigan 48823. Supported by the National Science Foundation.

‡Present address: Center for Nuclear Studies, University of Texas, Austin, Texas.

[1]C. F. Moore, C. E. Watson, S. A. A. Zaidi, J. J. Kent, and J. G. Kulleck, Phys. Rev. Letters 17, 926 (1966).

[2]W. R. Coker and T. Tamura, Phys. Rev. 182, 1277 (1969).

[3]R. A. Hinrichs, G. W. Phillips, J. G. Cramer, and H. Wieman, Phys. Rev. Letters 22, 301 (1969).

[4]L. S. Michelman, T. I. Bonner, and J. G. Kulleck, Phys. Letters 28B, 659 (1969).

[5]S. A. A. Zaidi and P. von Brentano, Phys. Letters 23, 466 (1966).

[6]T. Tamura and C. E. Watson, Phys. Letters 25B, 186 (1967).

[7]F. Karasek, Microfoils, Argonne, Illinois.

[8]P. Fessenden, W. R. Gibbs, and R. B. Leachman, Phys. Rev. Letters 15, 796 (1965).

[9]J. P. Bondorf, C. Ellegaard, J. Kantele, H. Lutken, and P. Vedelsby, Nucl. Phys. A101, 338 (1967).

[10]G. Friedman, A. Ginzbing, A. A. Jaffee, and A. Marinov, Nucl. Phys. A110, 300 (1968).

[11]E. W. Hamburger, Phys. Rev. Letters 19, 36 (1967).

[12]R. G. Clarkson, Ph.D. thesis, University of Texas, 1969 (unpublished).

[13]R. Heffner, C. Ling, N. Cue, and P. Richard, Phys. Letters 26B, 150 (1968).

[14]C. F. Moore, Phys. Letters 25B, 408 (1967).

[15]R. G. Clarkson and W. R. Coker, Phys. Rev. C 2, 1108 (1970).

[16]A. M. Lane, Phys. Letters 33B, 274 (1970).

[17]C. E. Watson, E. F. Alexander, and W. N. Shelton, Bull. Am. Phys. Soc. 12, 1196 (1967).

[18]W. R. Coker and C. F. Moore, Bull. Am. Phys. Soc. 13, 631 (1968).

[19]W. R. Coker and C. F. Moore, Phys. Letters 25B, 271 (1967).

[20]S. A. A. Zaidi, W. R. Coker, and D. G. Martin, Phys. Rev. C 2, 1364 (1970).

[21]M. Cosack, M. K. Leung, M. T. McEllistrem, R. L. Schulte, M. M. Stautberg, J. L. Weil, and J. C. Norman, Nucl. Phys. A136, 532 (1969).

[22]L. S. Michelman and C. F. Moore, Phys. Letters 26B, 446 (1968).